

## Lifetime Measurement of ${}_{\Lambda}^{12}\text{C}$ , ${}_{\Lambda}^{28}\text{Si}$ , and ${}_{\Lambda}\text{Fe}$ Hypernuclei

H. Bhang,<sup>1</sup> S. Ajimura,<sup>5</sup> K. Aoki,<sup>3</sup> T. Hasegawa,<sup>4,\*</sup> O. Hashimoto,<sup>2</sup> H. Hotchi,<sup>4</sup> Y. D. Kim,<sup>1,3,†</sup> T. Kishimoto,<sup>5</sup>  
K. Maeda,<sup>2</sup> H. Noumi,<sup>3</sup> Y. Ohta,<sup>4</sup> K. Omata,<sup>3</sup> H. Outa,<sup>3</sup> H. Park,<sup>1</sup> Y. Sato,<sup>2</sup> M. Sekimoto,<sup>3</sup> T. Shibata,<sup>3</sup>  
T. Takahashi,<sup>2</sup> and M. Youn<sup>1,2,‡</sup>

<sup>1</sup>Department of Physics, Seoul National University, Seoul 151-742, Korea

<sup>2</sup>Physics Department, Tohoku University, Sendai 980-8578, Japan

<sup>3</sup>High Energy Accelerator Research Organization (KEK), Tsukuba, Ibaraki 305-0801, Japan

<sup>4</sup>Graduate School of Science, University of Tokyo, Tokyo 113-0033, Japan

<sup>5</sup>Department of Physics, Osaka University, Toyonaka, Osaka 560-0043, Japan

(Received 27 July 1998)

We have measured lifetimes of  $\Lambda$  hypernuclei over a broad mass range explicitly identifying  $\Lambda$  hypernuclear production in the  $(\pi^+, K^+)$  reaction. The obtained results are  $\tau({}_{\Lambda}^{12}\text{C}) = 231 \pm 15$  ps,  $\tau({}_{\Lambda}^{28}\text{Si}) = 206 \pm 12$  ps, and  $\tau({}_{\Lambda}\text{Fe}) = 215 \pm 14$  ps. The lifetimes of  $\Lambda$  hypernuclei over the mass region from carbon to iron are found almost constant at about 80% of that of free  $\Lambda$  within the statistical uncertainties. The short-range nature of the nonmesonic weak decay process, which is dominant in heavy  $\Lambda$  hypernuclei, is possibly responsible for the observed weak hypernuclear mass dependence. [S0031-9007(98)07604-2]

PACS numbers: 21.80.+a, 13.30.Eg, 13.75.Ev, 21.10.Tg

A  $\Lambda$  hyperon bound in a nucleus eventually decays from the ground state either through a  $\pi$ -mesonic or a non-mesonic weak decay (NMWD) process. Through a  $\pi$ -mesonic process, a  $\Lambda$  in a hypernucleus decays to a nucleon and a pion, i.e.,  $\Lambda \rightarrow N\pi$ , as a free  $\Lambda$  does. However, the  $\pi$ -mesonic decay is strongly suppressed in hypernuclei, except very light ones, due to the small energy release in the process and the Pauli blocking. Instead, the NMWD process, which is the strangeness changing baryon-baryon weak interaction process ( $\Lambda + N \rightarrow N + N$ ), becomes dominant in most hypernuclei due to the much larger momentum of the final nucleon,  $\sim 400$  MeV/ $c$ , than the typical Fermi momentum,  $\sim 270$  MeV/ $c$ .

The total decay width of a  $\Lambda$  hypernucleus,  $\Gamma$ , is the sum of the partial decay widths;

$$\Gamma (= 1/\tau) = \Gamma_{\pi} + \Gamma_{nm} = \Gamma_{\pi} + \Gamma_p + \Gamma_n (+\Gamma_{2p2h}), \quad (1)$$

where  $\tau$  is a lifetime. Here, the  $\Gamma_{\pi}$  and  $\Gamma_{nm}$  are the partial decay widths for  $\pi$ -mesonic decay and NMWD, respectively.  $\Gamma_p$  and  $\Gamma_n$  are the partial widths for  $\Lambda + p \rightarrow n + p$  and  $\Lambda + n \rightarrow n + n$ , respectively, and  $\Gamma_{2p2h}$  is that of two-nucleon-induced NMWD ( $\Lambda NN \rightarrow NNN$ ). The branching ratio for the NMWD process already reaches to about 3/4 by  ${}_{\Lambda}^{12}\text{C}$  [1,2]. Therefore, the decay of heavy  $\Lambda$  hypernuclei provides us with valuable and clean information on the NMWD process, henceforth the baryon-baryon weak interaction and the short-range correlations in nuclear matter.

However, the understanding of the NMWD process is still in a primitive stage. Although there have been several microscopic model calculations for NMWD processes, which are based on either various meson exchange interactions [3–5] or quark-hadron hybrid interactions [6,7], none

of them have successfully reproduced both the total ( $\Gamma$ ) and partial decay widths ( $\Gamma_n$  and  $\Gamma_p$ ) simultaneously and particularly their ratio ( $\Gamma_n/\Gamma_p$ ).

So far the experimental data for the partial decay widths had large errors and provided only limited constraints. Among the weak decay observables, the lifetime can be determined most accurately free from nuclear final state interactions and material effects. Therefore its accurate data for heavy  $\Lambda$  hypernuclei are very much awaited to understand the NMWD mechanism.

The most reliable measurements of hypernuclear lifetimes were carried out for relatively light hypernuclei from  ${}_{\Lambda}^4\text{H}$  [8] to  ${}_{\Lambda}^{12}\text{C}$  [9] by direct measurements of the production and decay times of the  $\Lambda$  hypernuclei. There have been a few other lifetime measurements for heavier  $\Lambda$  hypernuclei [10–13]. However, in these measurements the produced hypernuclei were not explicitly identified. The reliable measurement for heavier hypernuclear lifetime would help to see the effect of the nuclear medium on the lifetime and to understand NMWD process.

In the present paper, we report on the lifetime measurement of  $\Lambda$  hypernuclei in the mass range from carbon to iron by the direct time measurement with explicit identification of the produced  $\Lambda$  hypernuclei. The  $(\pi^+, K^+)$  reaction was employed in the present experiment instead of the  $(K^-, \pi^-)$  reaction since it has the advantage to populate bound hypernuclear states [14,15] and give a virtually background-free spectrum [16] particularly for heavier  $\Lambda$  hypernuclei. The experiment was carried out at the K6 beam line of the KEK 12 GeV PS with 1.05 GeV/ $c$  pion beam for three targets: C, Si, and Fe.

The production of hypernuclear bound states by the  $(\pi^+, K^+)$  reaction was identified by using the good-resolution, large-acceptance, scattered-particle spectrometer SKS (superconducting kaon spectrometer), whose

intrinsic momentum resolution was better than  $10^{-3}$  and whose solid angle was  $\sim 100$  msr [17]. Because of the good momentum resolution and the cleanness of the  $(\pi^+, K^+)$  spectrum, we were able to separate the ground states of  ${}_{\Lambda}^{12}\text{C}$  and  ${}_{\Lambda}^{28}\text{Si}$  reasonably well, even though the targets were thick.

A schematic drawing of the target region is shown in Fig. 1. A plastic scintillator ( $T_1$ ) was installed just before the target to determine the beam timing. Targets were tilted by about  $9^\circ$ – $13^\circ$  with respect to the beam not only to minimize energy thresholds for decay protons and pions but also to make the targets thick along the beam, that is, 6.4(C), 10.3(Si), and 7.0(Fe) g/cm<sup>2</sup>.

Protons and pions emitted in the weak decay process of the  $\Lambda$  hypernuclei were measured in coincidence with  $K^+$  detected by SKS by two coincidence detector systems placed symmetrically above and below the target. Each detector system, covering about 15% of the whole solid angle, consisted of a decay product timing counter ( $T_2$ ), a drift chamber, a range counter, and a veto counter. The center of  $T_2$  was located 3.7 cm from the center of the target.

The lifetimes were obtained from delayed time ( $t_d$ ) spectra for protons measured in coincidence with hypernuclear production by setting gates on peaks or on a region in the hypernuclear excitation energy spectrum as follows.

$$t_d = (T_2 - \text{TOF}_2) - (T_1 + \text{TOF}_1). \quad (2)$$

$T_1$  and  $T_2$  are the timing readouts from the beam ( $\pi^+$ ) timing and the decay product (proton) timing counters whose intrinsic resolutions are  $\sigma_{T_1} \approx 50$  ps and  $\sigma_{T_2} \approx 35$  ps [18].  $\text{TOF}_1$  and  $\text{TOF}_2$  are the flight times between the target and  $T_1$  or  $T_2$  counters.

In order to determine  $\text{TOF}_1$  and  $\text{TOF}_2$ , the trajectory and energy of the flight particle should be measured accurately. For the trajectory measurement, drift chambers were installed between the timing counter  $T_2$  and the range counters, as shown in Fig. 1. The spatial resolution was about 0.35 mm. For the energy measurement, two sets of range counters composed of 20 layers of scintillators with a total thickness of 10 cm were installed. A typical energy resolution was about 2 MeV for normally

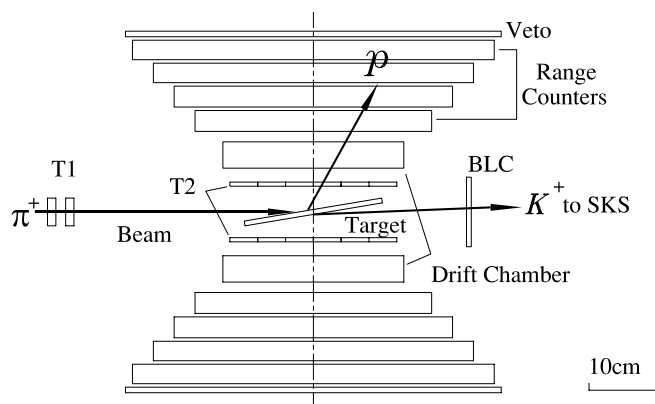


FIG. 1. A schematic view of the coincidence detector system used for the lifetime measurements of hypernuclei.

incident protons of  $\sim 100$  MeV. A veto counter was used to reject high-energy particles which were not stopped in the range counter. The energy ranges covered were 30–140 MeV for protons and 12–70 MeV for pions.

Particle identification (PID) of decay products was made by the  $\Delta E$ -range method. The light output from a  $T_2$  (6 mm thick scintillator) counter was used for  $\Delta E$ . The PIDs obtained for  $p$  and  $\pi$  were good enough, and the intermixing between  $p$  and  $\pi$  groups was less than 2% [19].

Figure 2(a) shows the excitation energy spectra for  ${}_{\Lambda}^{12}\text{C}(\pi^+, K^+)_{\Lambda}^{12}\text{C}$  gated with PID windows for  $p$  and  $\pi$ . The solid and dotted lines are  $p$ -gated and  $\pi$ -gated spectrum, respectively. The  $1s$  and the  $1p$   $\Lambda$  single particle states in the  $p$ -gated spectrum were reasonably well resolved. The gated region for the delayed time ( $t_d$ ) determination of  ${}_{\Lambda}^{12}\text{C}$  is indicated with an arrow in Fig. 2(a). The  $\pi$ -gated spectrum is dominated by the quasifree pionic decay in which  $\pi^+$ 's are produced from the decays of unbound  $\Lambda$ 's. This can be clearly seen from the rise of  $\pi$  spectrum around  $B_{\Lambda} = 0$ . Similarly Figs. 2(b) and 2(c) show the  $p$  and  $\pi^-$  gated spectra for  ${}_{\Lambda}^{28}\text{Si}$  and  ${}_{\Lambda}^{56}\text{Fe}$ . For  ${}_{\Lambda}^{28}\text{Si}$  we again gated for the  $1s$   $\Lambda$  ground state. For  ${}_{\Lambda}^{56}\text{Fe}$ , the ground state peak was no longer separable, but the hypernuclear bound states were clearly identified and integrated to obtain the lifetime. We note that the  $\Lambda$  bound region of  ${}_{\Lambda}^{56}\text{Fe}$  is open for particle decay channels. Therefore, some of the  $\Lambda$  bound  ${}_{\Lambda}^{56}\text{Fe}$  states first decay through particle emissions and eventually reach a ground state of a nearby hypernucleus where the  $\Lambda$  undergoes a weak decay. The  $\Lambda$  hypernuclei reached via

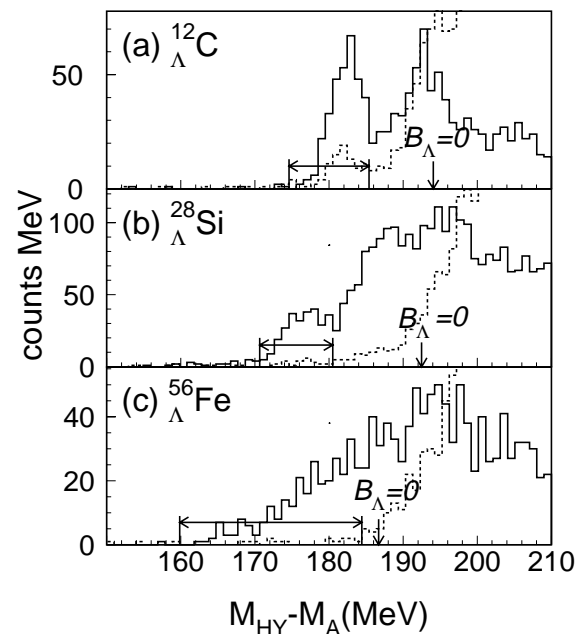


FIG. 2. The hypernuclear mass spectra for (a)  ${}_{\Lambda}^{12}\text{C}$ , (b)  ${}_{\Lambda}^{28}\text{Si}$ , and (c)  ${}_{\Lambda}^{56}\text{Fe}$  observed in coincidence with emitted protons (solid line) and pions (dotted line).  $M_{HY}$  and  $M_A$  are the masses of a hypernucleus and a target nucleus. The horizontal arrows represent the gate for the events used for the lifetime analyses.

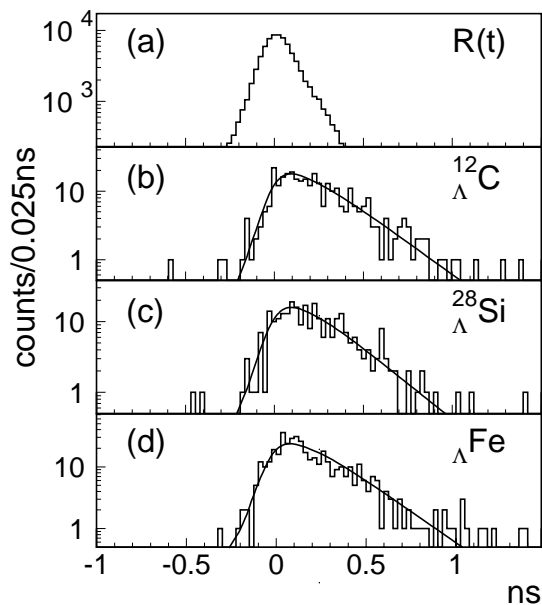


FIG. 3. The time spectra ( $t_d$ ) for (a) the prompt events of  $(\pi^+, 2p)$ , the hypernuclear weak decay events of (b) the ground state of  ${}^{12}_{\Lambda}\text{C}$ , (c) the ground state of  ${}^{28}_{\Lambda}\text{Si}$ , and (d) the whole bound states of  ${}_{\Lambda}\text{Fe}$  are shown.

particle decays will be in the mass region of  $54 \leq A \leq 56$ . (They are denoted as  ${}_{\Lambda}\text{Fe}$ .) The integrated bound region is indicated by an arrow. The pion coincidence spectrum rises sharply at the  $\Lambda$  binding threshold, and very few events remain below the gate channel in the pion coincidence spectrum. This demonstrates that the integrated region of the  $\Lambda$  bound states in  ${}_{\Lambda}\text{Fe}$  were properly selected.

To obtain prompt time response,  $(\pi^+, 2p)$  events were recorded simultaneously with  $(\pi^+, K^+)$  events. One proton was identified by the SKS spectrometer through the same procedure as the kaon, and the other was analyzed by one of the coincidence detector systems. Figure 3(a) shows a typical  $(\pi^+, 2p)$  time spectrum for the  ${}^{12}\text{C}$  target. The timing resolution was about 85 ps in  $\sigma$  which was much smaller than the typical lifetime,  $\tau \sim 200$  ps, so that the error of the measured lifetime was not limited by this resolution, but by the statistics.

Figures 3(b)–3(d) show the delay time spectra of  ${}^{12}_{\Lambda}\text{C}$ ,  ${}^{28}_{\Lambda}\text{Si}$ , and  ${}_{\Lambda}\text{Fe}$ , respectively, obtained by Eq. (2). The gated excited region for each case and the number of events are listed in Table I. To extract the lifetime, the delay time spectrum was fitted with the statistical distribution

$$D(t) = \int_0^{\infty} R(t - t') e^{-t'/\tau} dt', \quad (3)$$

which is a convoluted distribution of the exponential decay function with a response function,  $R(t)$ , which is the previously mentioned  $(\pi^+, 2p)$  time spectrum [Fig. 3(a)]. In the fitting procedure, we used the maximum likelihood method with Poisson statistics.

The lifetime ( $\tau$ ) results obtained from these spectra are

$$\tau({}^{12}_{\Lambda}\text{C}_{\text{g.s.}}) = 231 \pm 15 \text{ ps},$$

$$\tau({}^{28}_{\Lambda}\text{Si}_{\text{g.s.}}) = 206 \pm 12 \text{ ps},$$

$$\text{and } \tau({}_{\Lambda}\text{Fe}) = 215 \pm 14 \text{ ps},$$

where the errors are statistical. The present result for  ${}^{12}_{\Lambda}\text{C}$  is consistent with the previous one from BNL [9] within 1 standard deviation, but provides a reduced uncertainty by a factor of 2 due to the improved statistics. In Table I, the present results for the lifetimes and the total decay widths are listed, together with the previous measurements [10–13]. We have examined, on the systematic errors in our measurement from the dependence on the decay particle energy, the difference between up and down coincidence detector systems and the contamination from the higher excited energy states. No significant systematic error was found.

In Fig. 4, the present results of the lifetimes for  ${}^{12}_{\Lambda}\text{C}$ ,  ${}^{28}_{\Lambda}\text{Si}$ , and  ${}_{\Lambda}\text{Fe}$  (closed circles) are compared with the previous data (open circles) obtained from counter experiments with explicit identifications of the produced  $\Lambda$  hypernuclei. The horizontal error bar for the  ${}_{\Lambda}\text{Fe}$  data represents the mass range of the hypernuclei where weak decays take place. One does not, however, expect much variation of the lifetime in this mass range because the NMWD process, which is dominant, should not be very sensitive to an outmost valence nucleon distribution of the hypernucleus. The observed lifetimes of  $\Lambda$  hypernuclei, over the mass range of  $12 \leq A \leq 56$ , are almost constant (saturated) as

TABLE I. Present results (bold characters) for the lifetimes and the total decay widths of  $\Lambda$  hypernuclei are listed, together with the previous lifetime measurements for the medium and heavy hypernuclei.

	Gate window (MeV)	Number of events	Lifetime (ps)	$\Gamma$ ( $\Gamma_{\Lambda}$ )
${}^{12}_{\Lambda}\text{C}$	175–186	323	<b>231 ± 15</b>	<b>1.14 ± 0.08</b>
${}^{\sim 16}_{\Lambda}\text{Z}$	...	...	$86^{+33}_{-26}$ [10]	...
${}^{28}_{\Lambda}\text{Si}$	171–181	527	<b>206 ± 12</b>	<b>1.28 ± 0.08</b>
${}_{\Lambda}\text{Fe}$	160–185	309	<b>215 ± 14</b>	<b>1.22 ± 0.08</b>
$\bar{p} + {}^{209}\text{Bi}$	...	...	180 ± 72 [12]	...
$\bar{p} + {}^{238}\text{U}$	...	...	130 ± 42 [12]	...
$p + {}^{238}\text{U}$	...	...	240 ± 60 [13]	...

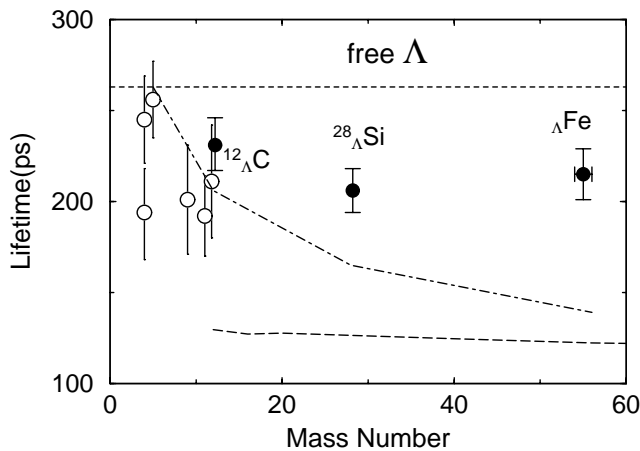


FIG. 4. The mass dependence of the hypernuclear lifetimes. The present results (closed circles) are compared with the previous ones (open circles). The dotted line represents the lifetime of a free  $\Lambda$ . The dot-dashed line is the calculation of Itonaga *et al.* and the dashed one of Ramos *et al.*

about 80% of the free  $\Lambda$  value. The lifetimes of  $^{28}_{\Lambda}\text{Si}$  and  $_{\Lambda}\text{Fe}$  are slightly shorter than that of  $^{12}_{\Lambda}\text{C}$ . However, their differences from the (saturated) constant value are within experimental uncertainties.

The dot-dashed line in Fig. 4 is the calculated mass dependence of the lifetime based on the one-pion and correlated two-pion exchange model of Itonaga *et al.* [20]. Although light  $\Lambda$  hypernuclear lifetimes are well reproduced up to  $^{12}_{\Lambda}\text{C}$ , it shows a mass dependence contrary to the present data, significantly underestimating the lifetime for the hypernuclei heavier than  $^{12}_{\Lambda}\text{C}$ . The dashed line is the calculation of Ramos *et al.* [21], which is based on one-pion exchange model and included two-nucleon-induced NMWD. The calculated values are much smaller than the experimental ones even for light nuclei.

Assuming the short rangeness of the nonmesonic weak decay process, which is dominant in hypernuclei of  $A \geq 10$ , one can employ a zero range approximation for a qualitative understanding. The nonmesonic weak decay widths will then be proportional to the overlap integral of wave functions of a nucleon and a  $\Lambda$ , and the hypernuclear lifetimes will be almost constant in the mass region beyond carbon where the overlap integrals almost saturate. A simple discussion of the weak mass dependence was also made recently by assuming the interaction is sufficiently short ranged and by counting the number of  $\Lambda N$  bonds responsible for the nonmesonic weak decay [22].

The present lifetime data apparently require us to take into account the short-range nature of the nonmesonic weak decay, which does not seem to be properly included in the current meson exchange model. A better treatment of the short-range nature of NMWD in  $\Lambda$  hypernuclei is very much awaited.

In summary, we have measured lifetimes for  $\Lambda$  hypernuclei:  $^{12}_{\Lambda}\text{C}$ ,  $^{28}_{\Lambda}\text{Si}$ , and  $_{\Lambda}\text{Fe}$ . The latter two, which are in the mass range beyond  $p$ -shell hypernuclei, were measured

for the first time explicitly identifying the produced  $\Lambda$  hypernuclear bound states. We observe that the lifetimes of  $\Lambda$  hypernuclei in the mass range heavier than 12 are almost mass independent. This weak mass dependence should be related to the mechanism of NMWD, which is dominant in the present mass region, and to the baryon-baryon short-range correlation inside the hypernucleus.

We are grateful for the generous support from the staff members of KEK and INS. We also deeply appreciate the continuous encouragement by Professor K. Nakai and Professor T. Yamazaki throughout this experiment from the beginning. We very much benefited from discussions with Professor K. Itonaga, Professor T. Motoba, Professor T. Fukuda, and Professor T. Nagae. H. B. acknowledges partial support from the Korea-Japan collaborative research program of KOSEF and from the Ministry of Education through the Research Institute of Basic Science at Seoul National University.

\*Present address: School of Allied Health Sciences, Kitasato University, Sagami-hara 228-8555, Japan.

†Present address: Department of Physics, Sejong University, Seoul 143-747, Korea.

‡Present address: University of Houston, Houston, Texas 77004.

- [1] H. Nouni *et al.*, Phys. Rev. C **52**, 2936 (1995).
- [2] A. Sakaguchi *et al.*, Phys. Rev. C **43**, 73 (1991).
- [3] J. B. Adams, Phys. Rev. **156**, 1611 (1967).
- [4] J. F. Dubach, Nucl. Phys. **A450**, 71c (1986).
- [5] A. Parreno, A. Ramos, and C. Bennhold, Nucl. Phys. **A585**, 129c (1995).
- [6] C. Y. Cheung, D. P. Heddle, and L. S. Kisslinger, Phys. Rev. C **27**, 335 (1983).
- [7] T. Inoue, S. Takeuchi, and M. Oka, Nucl. Phys. **A597**, 563 (1996).
- [8] H. Oota *et al.*, Nucl. Phys. **A547**, 109c (1992).
- [9] R. Grace *et al.*, Phys. Rev. Lett. **55**, 1055 (1985); J. J. Szymanski *et al.*, Phys. Rev. C **43**, 849 (1991).
- [10] K. J. Nield *et al.*, Phys. Rev. C **13**, 1267 (1976).
- [11] J. P. Bocquet *et al.*, Phys. Lett. B **182**, 146 (1986).
- [12] T. A. Armstrong *et al.*, Phys. Rev. C **47**, 1957 (1993).
- [13] H. Ohm *et al.*, Phys. Rev. C **55**, 3062 (1997).
- [14] P. H. Pile *et al.*, Phys. Rev. Lett. **66**, 2585 (1991).
- [15] T. Hasegawa *et al.*, Phys. Rev. C **53**, 1210 (1996).
- [16] T. Hasegawa *et al.*, Phys. Rev. Lett. **74**, 224 (1995).
- [17] T. Fukuda *et al.*, Nucl. Instrum. Methods Phys. Res., Sect. A **361**, 485 (1995).
- [18] Y. D. Kim *et al.*, Nucl. Instrum. Methods Phys. Res., Sect. A **372**, 431 (1996).
- [19] H. C. Bhang *et al.*, Nucl. Phys. **A639**, 269c (1998).
- [20] K. Itonaga, T. Ueda, and T. Motoba, Nucl. Phys. **A639**, 329c (1998).
- [21] A. Ramos, E. Oset, and L. Salcedo, Nucl. Phys. **A585**, 129c (1995).
- [22] K. Itonaga, in The Proceedings of the International Conference on Hypernuclear Spectroscopy, Sendai, 1998 (to be published).